Strange Quark as a probe for new physics in the Higgs sector

ECFA Higgs/Top/EW Workshop – April 20, 2022
Matthew Basso (University of Toronto),
On behalf of the authors of the associated Snowmass 2021 paper and the ILD Collaboration

UNIVERSITY OF TORONTO

SnowMass2021

Overview

- Broad interest in studying the light quark Yukawa couplings at future lepton colliders as a portal to BSM physics
  - See recent ECFA seminar on physics with light quarks
- Goal of this study: assess the sensitivity of Higgs to strange couplings at the ILC and to study detector design enabling *strange jet tagging*
  - Strange jet tagging capabilities strongly depend on particle identification (PID)
  - Submitted as part of the Snowmass 2021 proceedings: 2203.07535

Strange quark as a probe for new physics in the Higgs sector

Alexander Albert[a], Matthew J. Basso[b], Samuel K. Bright-Thonney[a], Valentina M. M. Cairo[c,d], Chris Damerell[e], Daniel Egaña-Ugrinovic[f], Ulrich Einhaus[g], Ulrich Heintz[h], Samuel Homiller[i], Shin-ichi Kawada[g], Jingyu Luo[h], Chester Mantel[j], Patrick Meade[k], Jose Monroy[a], Meenakshi Narain[h], Robert S. Orr[c], Joseph Reichert[a], Anders Ryd[a], Jan Strube[j], Dong Su[c], Ariel G. Schwartzman[c], Tomohiko Tanabe[l], Junping Tian[m], Emanuele Usai[h], Jerry Va'vra[c], Caterina Vernieri[c], Charles C. Young[c], and Rui Zou[a]

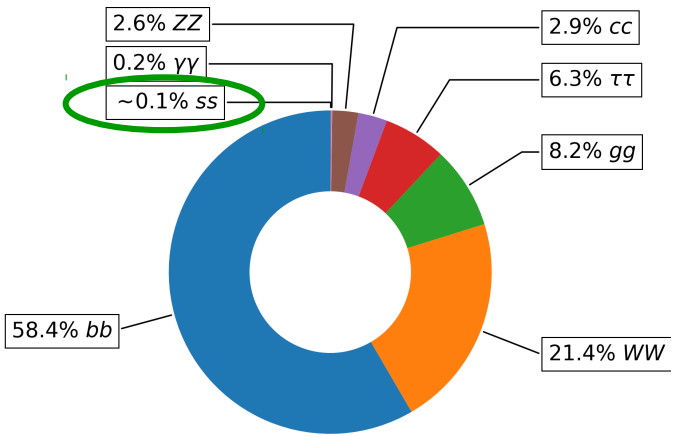

$\sqrt{s}$ = 13 TeV, m_H = 125 GeV

Measurement prospects for Higgs to strange

- $h(125) \to ss$: extremely challenging (BR ~ 1E-4) unless enhanced relative to SM expectations
  - Is the Yukawa coupling universal between generations?
- $H^{\pm} \to cs$: some BSM models allow for the 1st and 2nd generation fermion masses to be an additional source of EW symmetry breaking
  - Results in “SM” and “heavy” Higgs doublets
  - Predicts an enhancement to Higgs cross section
  - Charged heavy Higgs can undergo flavour violating decays (e.g., *cs*) – ***slc*-tagging at future detectors can help...**

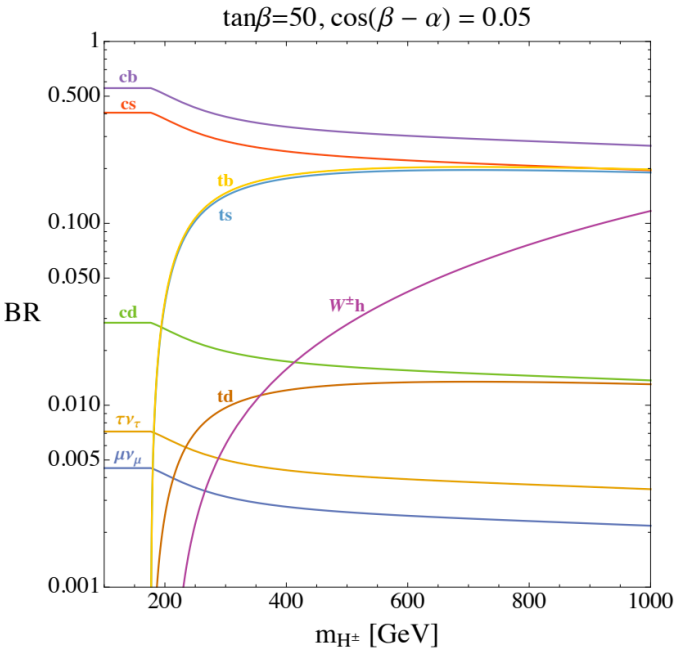

Charged heavy Higgs branching ratios. Taken from Fig. 6 of 1610.02398.

...one such proposed detector

- The International Large Detector (ILD)
  - 3 double-layer pixel detectors for vertexing
  - 2 double-layer pixel detectors, time projection chamber (TPC), and 1 double-layer strip detector for tracking
    - Low material of TPC assists in low-p tracking
  - Forward tracking detector provides tracking acceptance starting at $\theta = 4.8°$
  - High granularity sampling calorimeters for particle flow reconstruction
    - Precise EM/hadronic design still under study
  - Tracking/calorimetry contained in 3.5 (4) T field

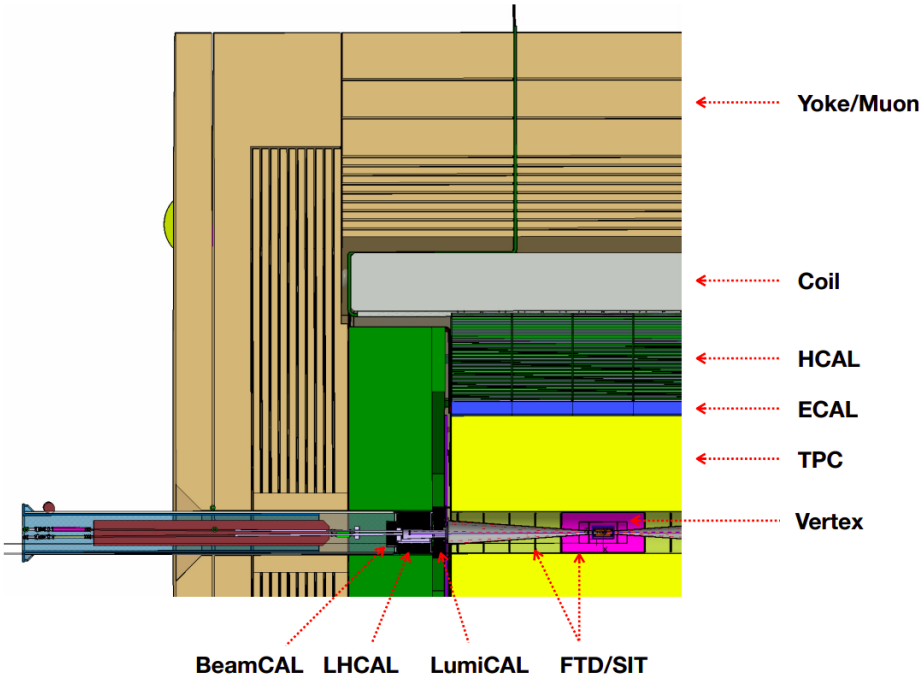

ILD detector quadrant. Taken from Fig. 5.1 of 2003.01116.

Developing a jet flavour tagger

- Developed a recurrent neural network for tagging jets by flavour, trained on ILD-reconstructed ($Z \to \nu\nu$)($h \to qq/gg$) samples
  - Architecture in Backup
- The tagger utilizes per-jet inputs and inputs for the 10 leading constituents in each jet
  - Includes 4-vector information and existing (LCFIPlus) jet tagger scores
  - Additionally use ***truth***-based PID inputs for the jet's constituents: electron, muon, proton, pion, or kaon (includes $K^{\pm}$, K_s^0, and Λ^0)

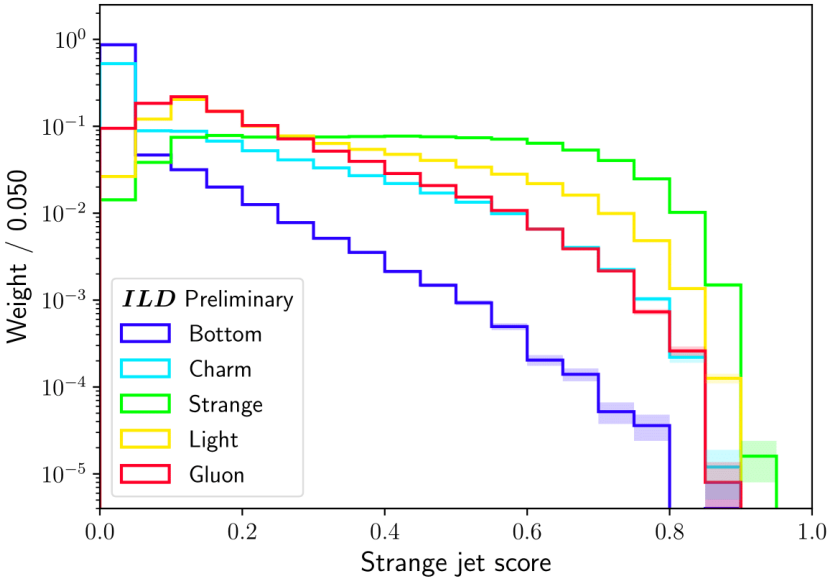

The tagger has 5 output nodes for gluon, light (u/d), strange, charm, and bottom jets. Pictured here is the strange node (others are in the Backup).

Standard Model *h*(125)→*ss* analysis

- Analysis measuring *Zh*(125)→*ss* at √*s* = 250 GeV using 900 fb^{-1} of data from the ILC's first 10 years of operation
- Performed in two channels based on the decay of the *Z*, *Z*→*νν* and *Z*→*ll*, each with their own dedicated selections
  - Leading backgrounds include *Z*→*qq* and semileptonic *Z*/*ZZ*
  - Full set of selections and backgrounds in Backup

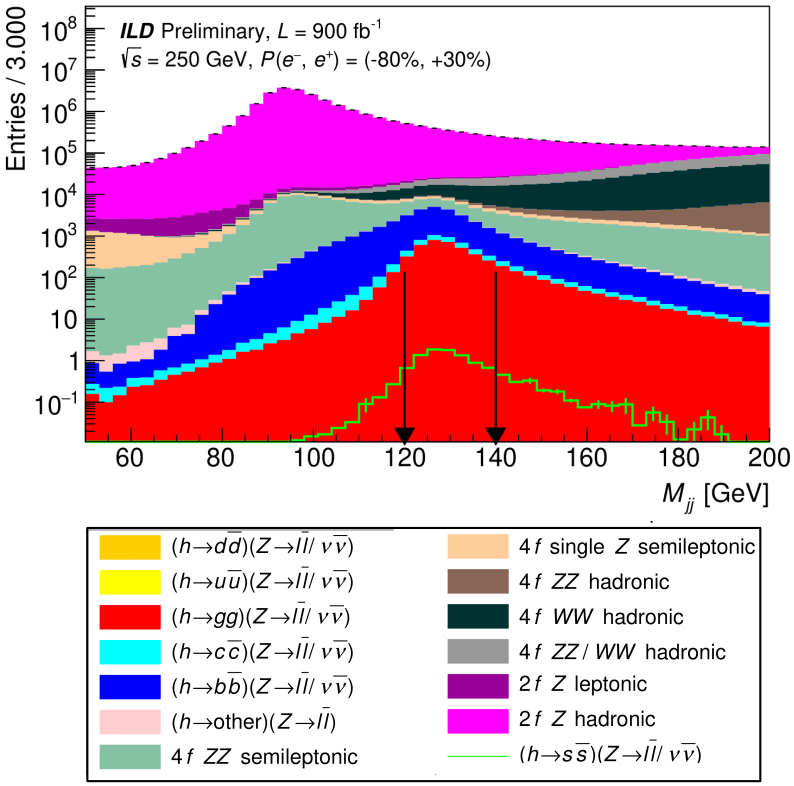

Combined limits on κ_s

$Z \to \nu\nu$ channel

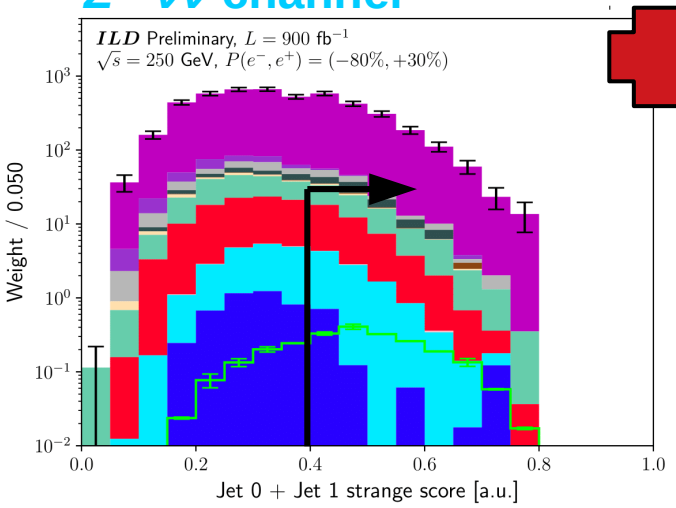

$Z \to ll$ channel

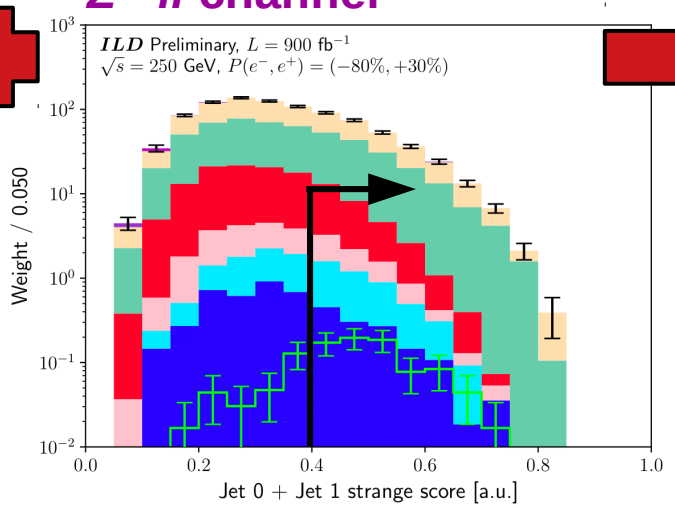

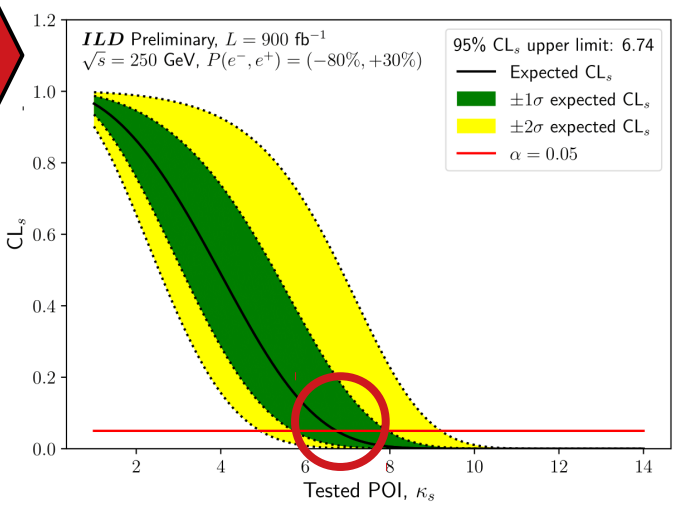

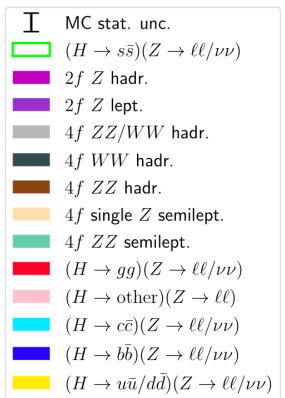

- A signal discriminant is constructed using the sum of the strange scores for the leading and subleading jets – yields a 2-bin fit
- Combined upper limit on the Higgs-strange Yukawa coupling modifier, κ_s, is found to be **6.7** – competitive with indirect searches (1905.03764)
  - Assumes uncertainties are dominated by *data statistics*

Constraining 2 Higgs doublet models

- Spontaneous flavour violating (SFV) 2HDMs allow for large Higgs-strange/light couplings
  - See 1908.11376, for instance
  - Can manifest as a modification of the SM Higgs-strange Yukawa coupling, due to mixing of the SM/BSM Higgs doublets
- Higgs to strange analyses at future lepton colliders stand to set some of the **strongest** limits on such models
  - Will improve even more when including the full ILC dataset and additional channels

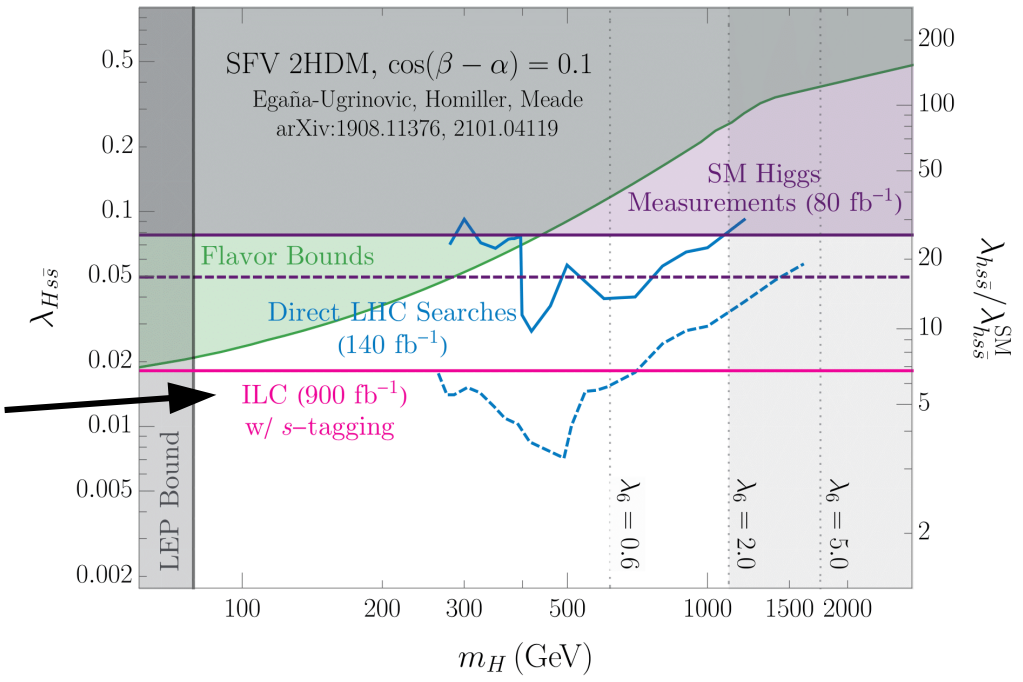

Dashed line := HL-LHC.

Particle identification is important!

- We can study the effect of having truth PID only up to certain particle momenta (0, 10, 20, 30, ∞ GeV)
- With no PID, there is **no** capacity for separating strange and light jets
  - At 80% light rejection, there is **~50% improvement** in strange efficiency going from PID < 10 GeV to PID < 30 GeV
- PID is ***essential*** for analyses studying strangeness (and specifically >10 GeV)

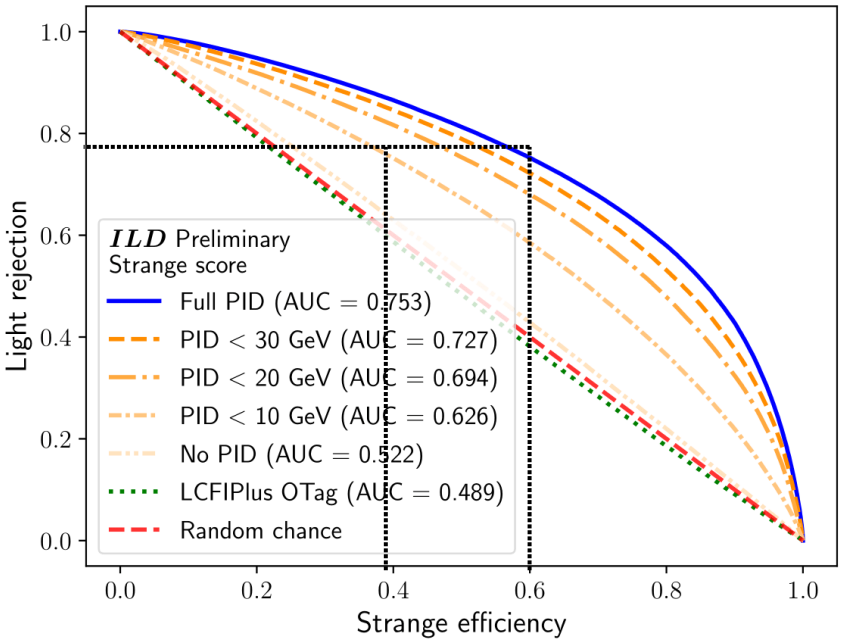

Detector proposal for high momentum PID

- Ring imaging Cherenkov (RICH) detectors: use the angle of emitted Cherenkov cones which, coupled with momenta measurements, yield particle masses
  - Used by DELPHI, SLD, LHCb...
- We are proposing the use of a *compact gaseous RICH detector* at future colliders
  - Also utilizes silicon photomultipliers (SiPMs)
  - **Benefits** include: π/K separation up to ~30 GeV, low material budget, low radial extent, ...

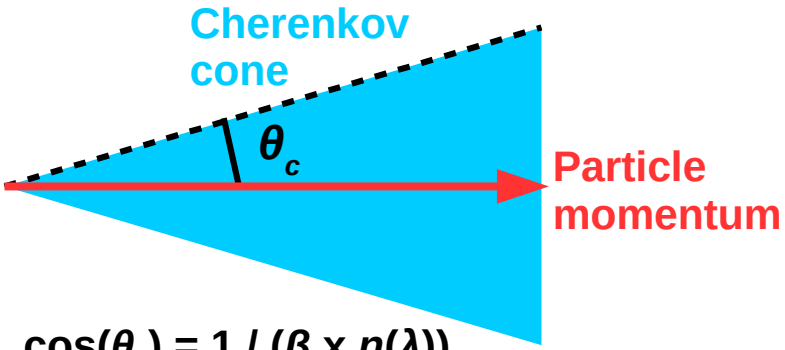

$\cos(\theta_c) = 1 / (\beta \times n(\lambda))$
θ_c := Cherenkov angle
β := v/c
n := refraction index

Compact gaseous RICH for ILD/SiD detectors

Pure C_4F_{10} at 1 bar (boiling point -1.9 °C at 1 bar) for radiator, ~flat refraction index in wavelength

Low-mass carbon-composite structure

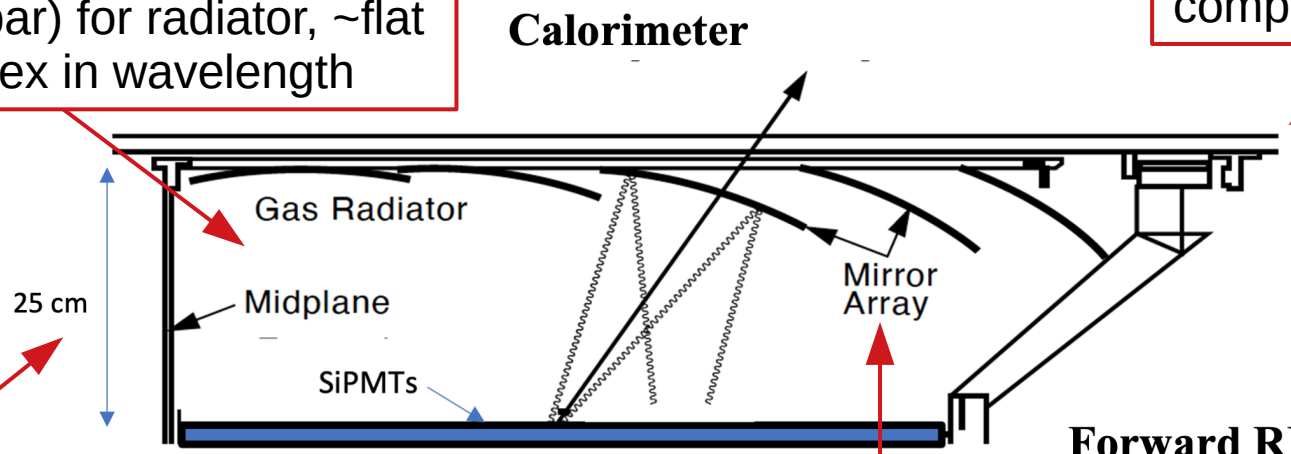

Small radial extent (helps reduce cost of the calorimeters)

SiPM imaging plane – broad quantum efficiency in wavelength, <100 ps timing resolution

Focusing mirrors made of Be with Cr/Al/MgF_2 coating, ~flat reflectivity in wavelength

Separation power for pions/kaons

- Achievable separation power for pions/kaons depends *strongly* on Cherenkov angle resolution
  - e.g., for our proposed RICH, resolutions **>5 mrad** degrade the performance significantly
- Different sources which contribute to the total resolution are enumerated in the Backup
  - **Particularly important is the magnetic smearing effect...**

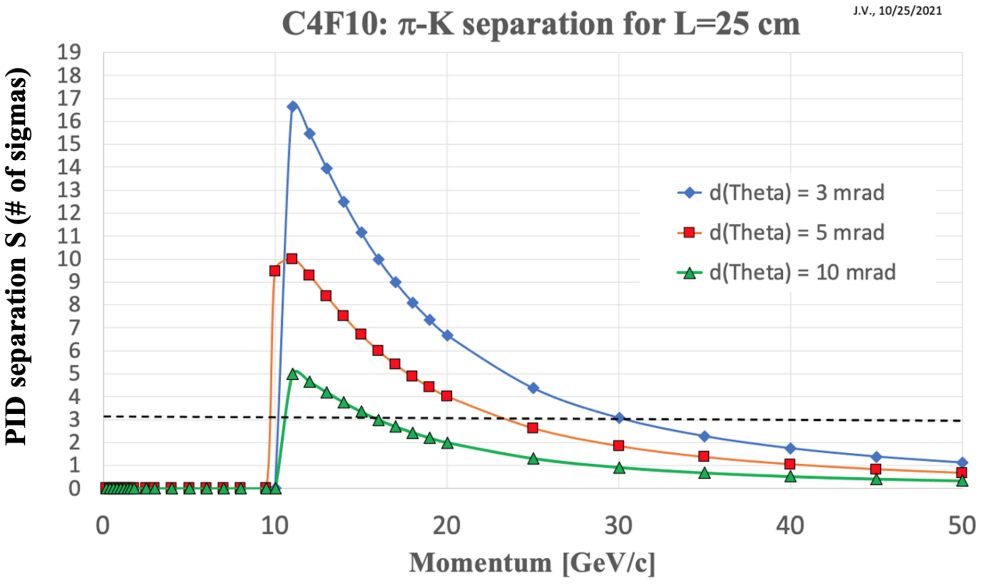

Separation power = $|\theta_\pi - \theta_K| \,/\, (\sigma_\theta \times \sqrt{N_{pe}})$
$\theta_{\pi(K)}$ = Cherenkov angle for pions (kaons)
σ_θ := Cherenkov angle resolution
N_{pe} := number of photoelectrons per ring

Magnetic smearing effect

- Cherenkov cones spiral in the magnetic field of the solenoid, leading to smeared images with elliptical shapes
  - Calculations assume **5 T** (comes from SiD design: 0911.0006)
  - **~2 mrad** contribution to the total resolution (**<5 mrad**)
- For a **50%** improvement in SiPM photon detection efficiency, the radiator length may be reduced to **10-15 cm**, reducing magnetic smearing

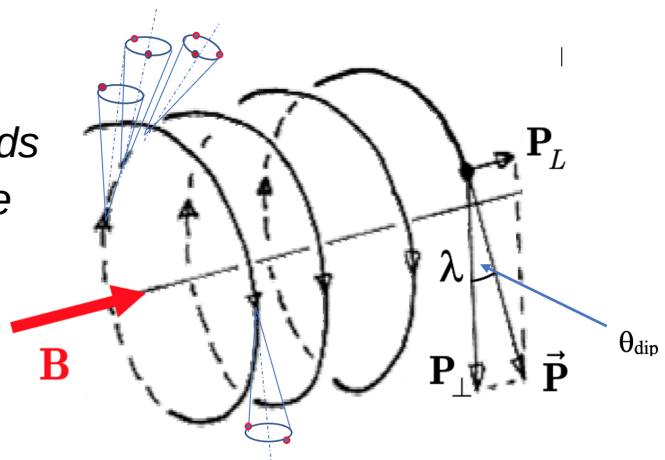

The dip angle θ_{dip} corresponds to the angle between particle momentum and component perpendicular to the field.

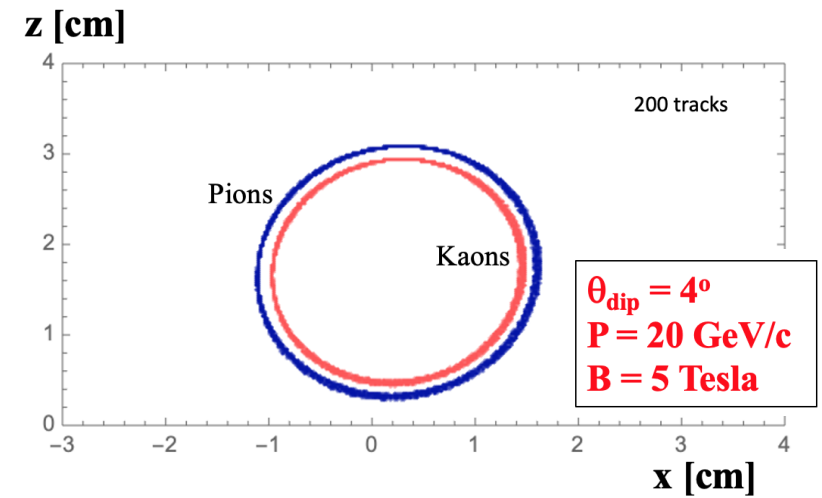

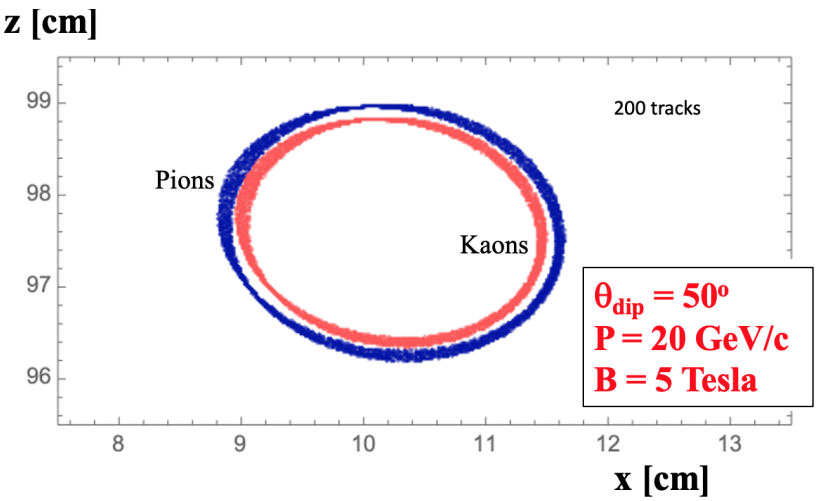

Summary and next steps

- Presented our studies towards strange tagging at future lepton colliders
  - Direct measurements of $h(125) \to ss$ at future colliders can provide competitive avenues for studying the extended Higgs sector – but PID is a necessary ingredient!
  - RICH detectors can offer >3σ pion/kaon separation up to ~30 GeV
    - *Cluster counting* in TPCs is also a powerful option (ILD: 1902.05519)
  - Ongoing: expanding to the full ILC luminosity, including $H^{\pm} \to cs$, and testing a modified ParticleNet (1902.08570) neural network for multiclassification
- Strange tagging broadly applicable to other measurements: $Z \to ss$, $e^+e^- \to ss$, $W \to cs$, ...
  - Prospect studies at the ILC and the FCC-ee are already examining at these channels

Questions?

Backup

Leading particle for jets of different flavours

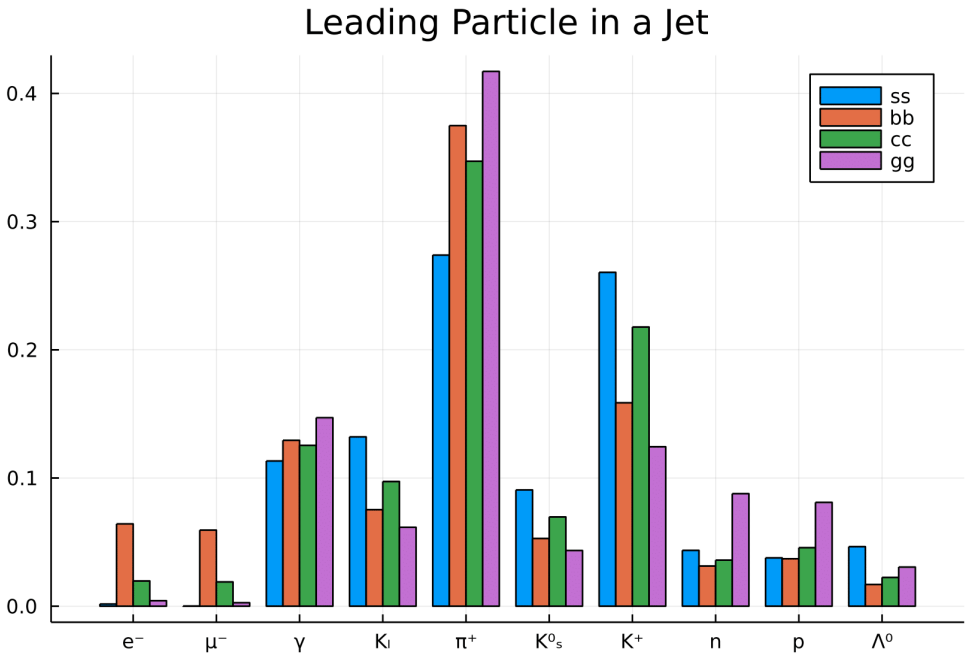

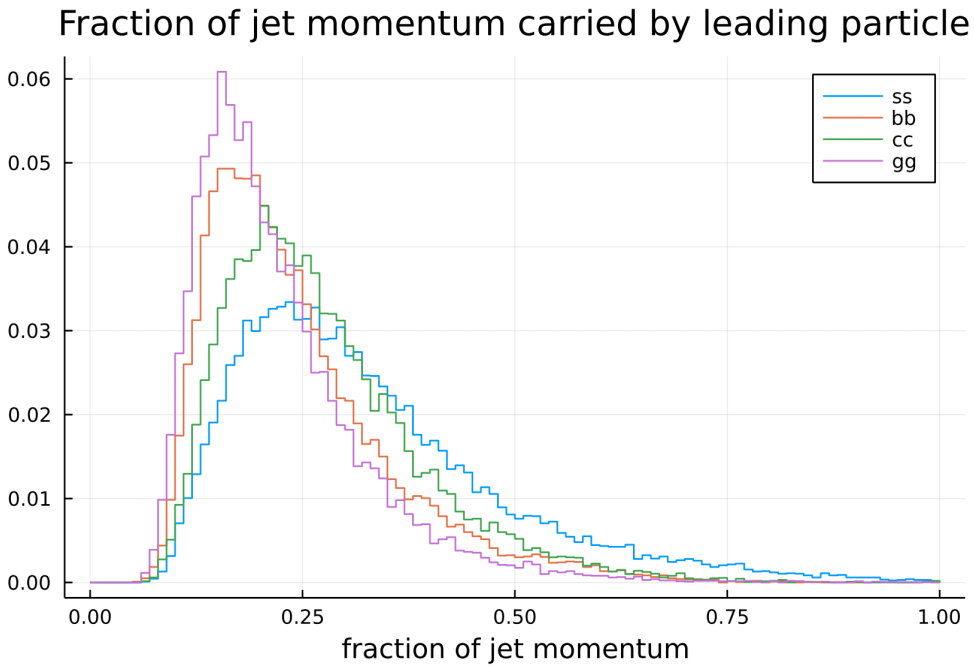

Jet flavour tagger architecture

- Neural network architecture:
  - *Multiclassifer* (5 output classes: gluon, light, strange, charm, or bottom)
  - 3-layer recurrent neural network using Gated Recurrent Units (GRUs) for particle-level inputs
  - Concatenated with jet-level inputs and fed into a 3-layer MultiLayer Perceptron (MLP)
  - Similar architecture applied for strange tagging at *hadron* colliders (2011.10736)

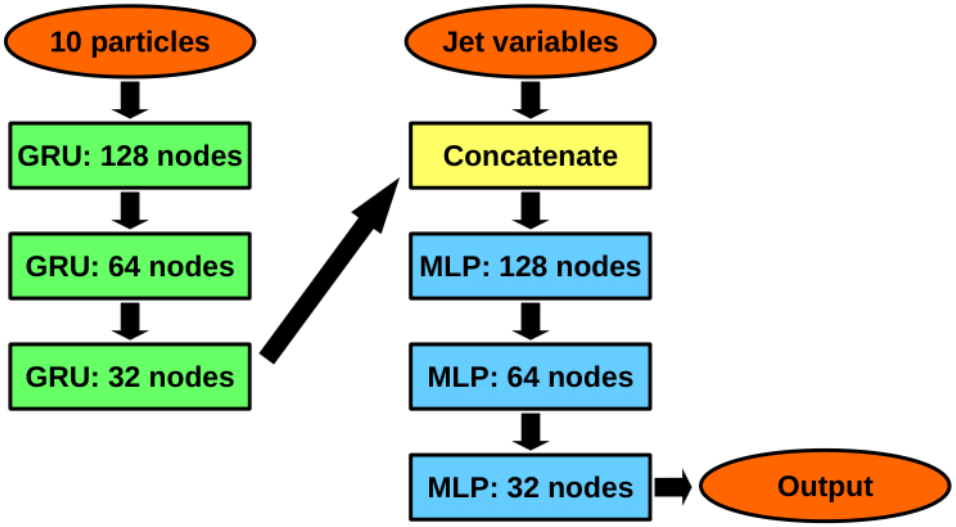

Jet flavour tagger output nodes

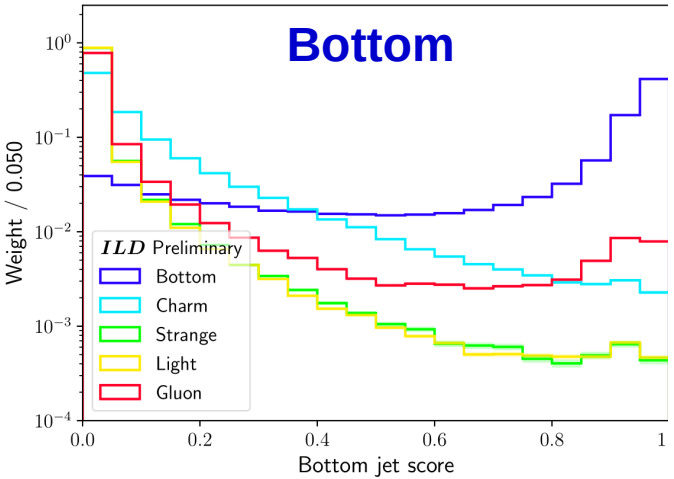

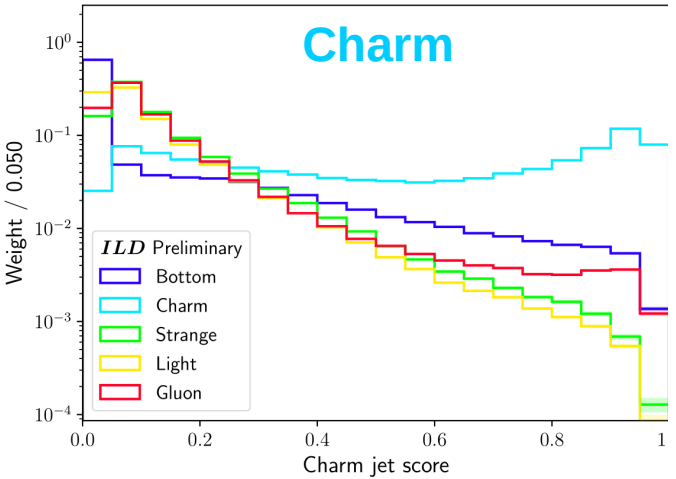

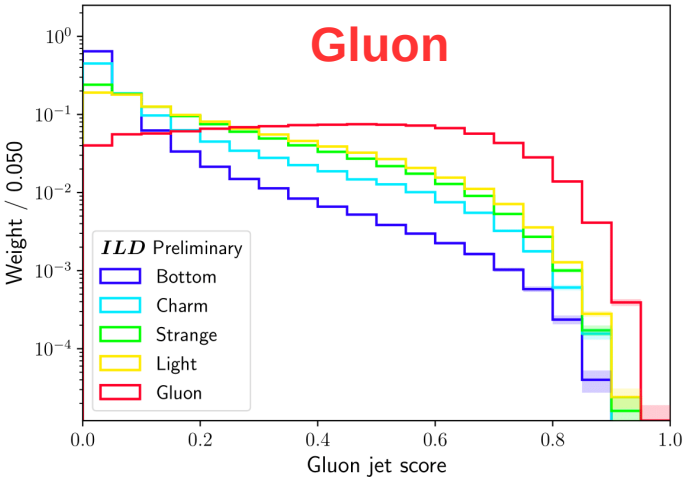

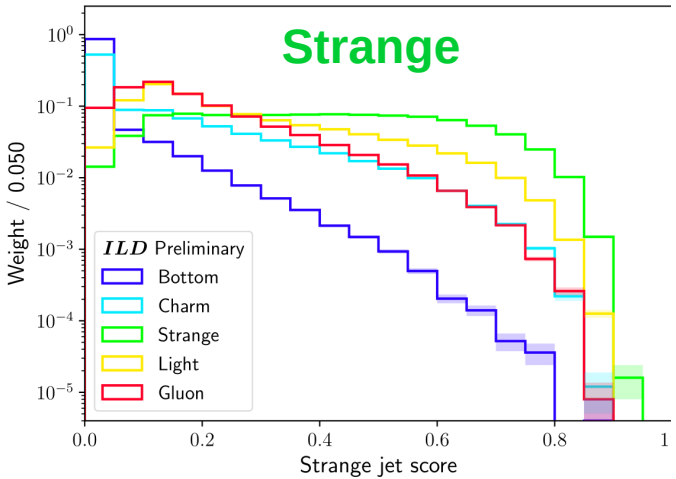

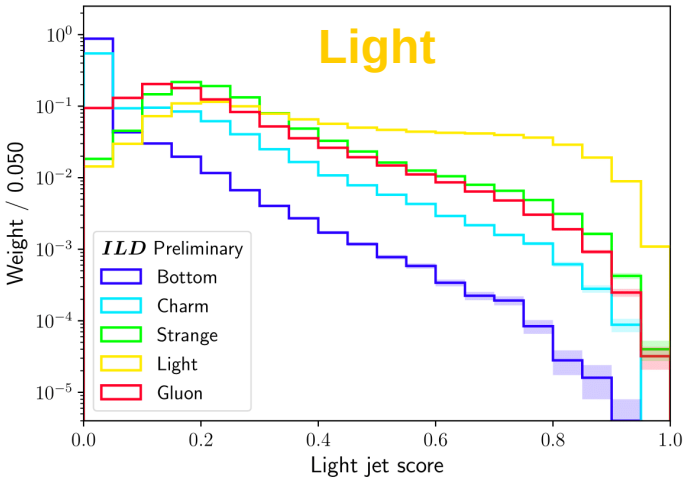

Confusion matrix for jet flavour tagger

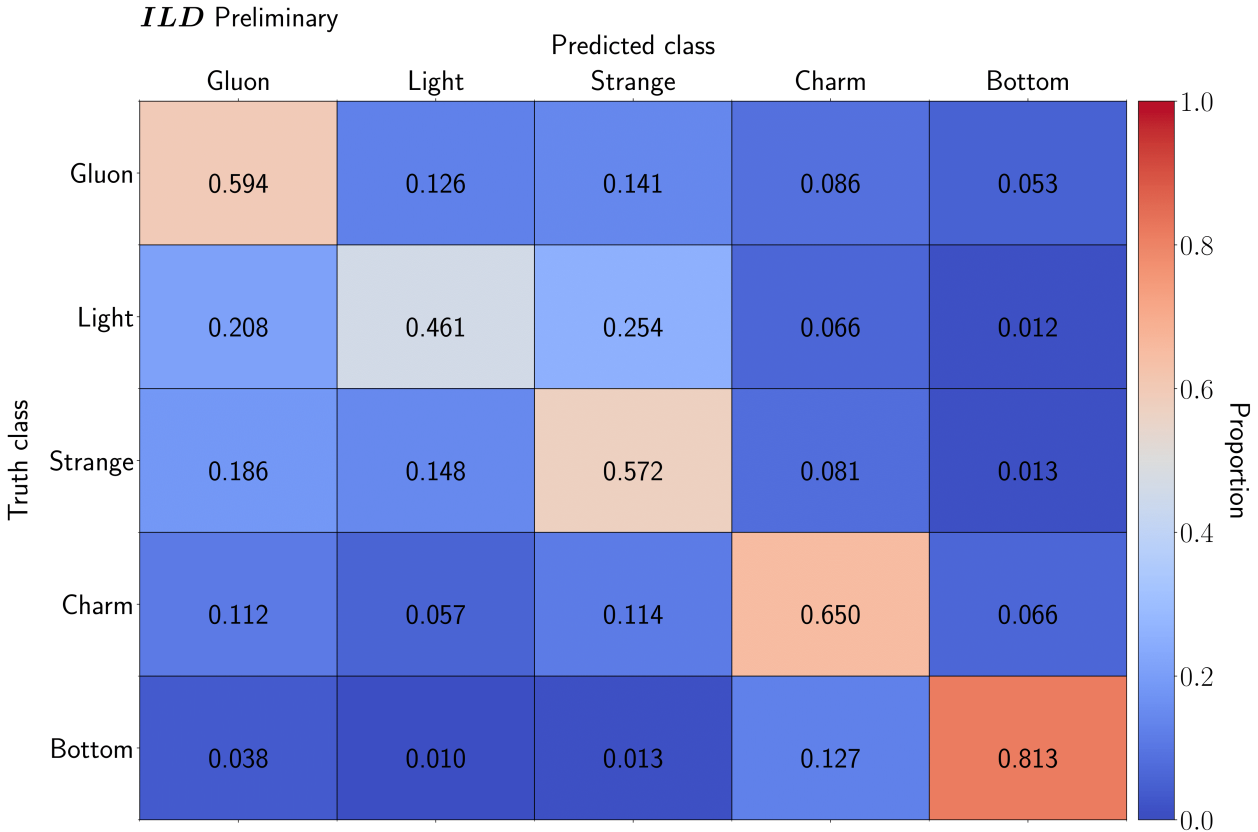

Leading strange hadron momentum for varying cuts on jet flavour tagger

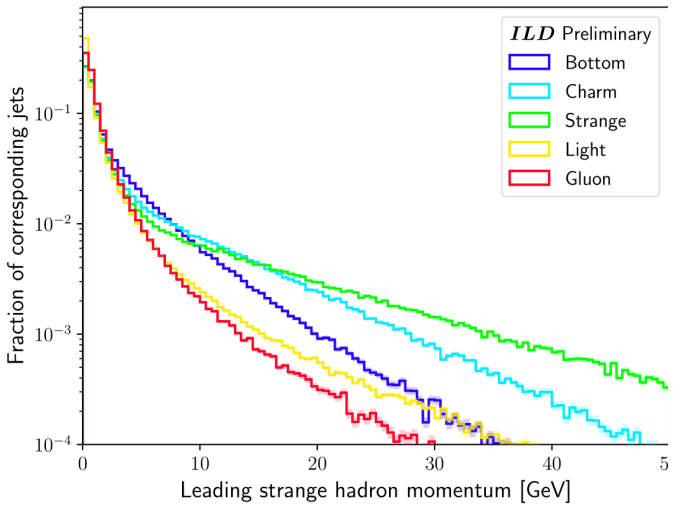

Strange score > 0.0

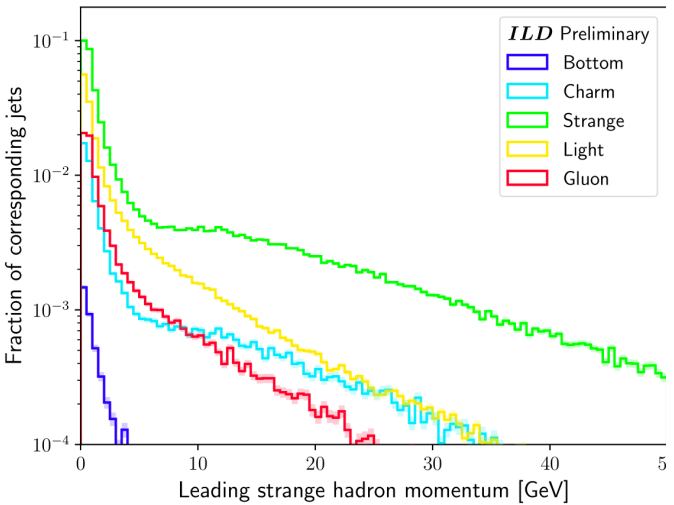

Strange score > 0.4

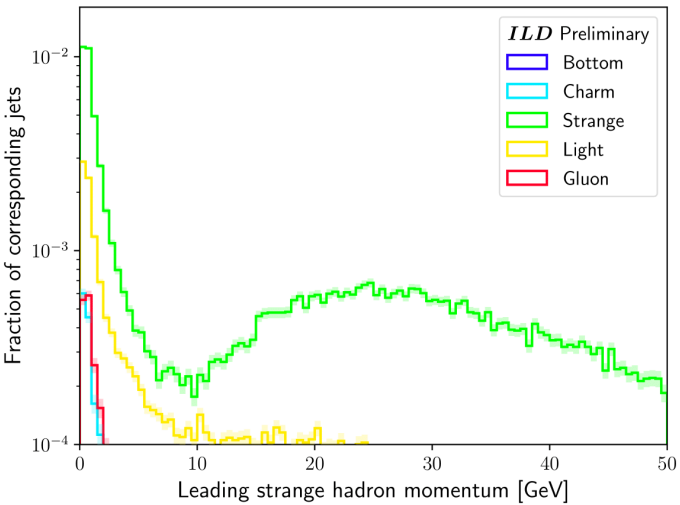

Strange score > 0.7

Cutting tighter on the strange output node selects jets with leading strange hadrons with higher momenta

MC samples and selections for $h \to ss$ analysis

Table 2: MC processes considered in the $h \to s\bar{s}$ analysis, including raw statistics and cross sections. N.B. the samples were generated at $\sqrt{s} = 250\,\text{GeV}$ and the cross sections assume 100% LH-polarised electron beams and 100% RH-polarised positron beams. The cross sections include the corresponding BRs for the indicated decays.[5] In the non-Higgs processes, "nf" denotes the number (n) of fermions (f) in the final state. In $Z(\to \ell\bar{\ell})h(\to \text{other})$, "other" denotes any non-hadronic SM decay. The $Z(\to \ell\bar{\ell})h(\to u\bar{u}/d\bar{d})$ processes, while having 0 raw events, have cross sections which are much smaller than that of $Z(\to \ell\bar{\ell})h(\to s\bar{s})$. Accordingly, they may be safely excluded from the analysis but are highlighted here for posterity. The ZZ/WW process covers the interference of ZZ and WW final states, e.g., $u\bar{u}d\bar{d}$ or $c\bar{c}s\bar{s}$.

Process name	Raw events [a.u.]	LR cross section [fb]
$Z(\to \nu\bar{\nu})h(\to s\bar{s})$	500,000	0.021
$Z(\to \nu\bar{\nu})h(\to b\bar{b})$	500,000	58.1
$Z(\to \nu\bar{\nu})h(\to c\bar{c})$	499,800	2.9
$Z(\to \nu\bar{\nu})h(\to u\bar{u})$	499,800	1×10^{-5}
$Z(\to \nu\bar{\nu})h(\to d\bar{d})$	500,000	5×10^{-5}
$Z(\to \nu\bar{\nu})h(\to gg)$	499,800	8.6
$Z(\to \ell\bar{\ell})h(\to s\bar{s})$	373	0.011
$Z(\to \ell\bar{\ell})h(\to b\bar{b})$	872,380	29.8
$Z(\to \ell\bar{\ell})h(\to c\bar{c})$	43,334	1.5
$Z(\to \ell\bar{\ell})h(\to u\bar{u})$	0	6×10^{-6}
$Z(\to \ell\bar{\ell})h(\to d\bar{d})$	0	3×10^{-5}
$Z(\to \ell\bar{\ell})h(\to gg)$	123,225	4.4
$Z(\to \ell\bar{\ell})h(\to \text{other})$	460,688	15.9
$2f$ Z hadronic	25,354,400	127,965
$4f$ ZZ hadronic	7,099,000	1,405
$4f$ WW hadronic	14,790,600	14,866
$4f$ ZZ/WW hadronic	18,494,200	12,389
$2f$ Z leptonic	24,500,000	21,214
$4f$ ZZ semileptonic	4,199,600	838
$4f$ single Z semileptonic	6,999,600	1,423

Table 3: Kinematic selections for $Z \to \nu\bar{\nu}$ and $Z \to \ell\bar{\ell}$ channels of the $h \to s\bar{s}$ analysis. The selections are grouped into categories serving specific purposes.

Category	Selection	$Z \to \nu\bar{\nu}$	$Z \to \ell\bar{\ell}$
Object counting	Number of leptons, N_{leptons}	0	≥ 2
	Number of jets, N_{jets}	≥ 2	≥ 2
	Leading 2 leptons are SFOS[8]	–	True
$2f$ Z rejection	Leading jet momentum, p_{j_0}	$\in [40, 110]\,\text{GeV}$	$\in [60, 105]\,\text{GeV}$
	Subleading jet momentum, p_{j_1}	$\in [30, 80]\,\text{GeV}$	$\in [35, 75]\,\text{GeV}$
	Dijet mass, M_{jj}	$\in [120, 140]\,\text{GeV}$	$\in [115, 145]\,\text{GeV}$
	Dijet energy, E_{jj}	$\in [125, 155]\,\text{GeV}$	$\in [130, 156]\,\text{GeV}$
	Missing mass, M_{miss}	$\in [75, 120]\,\text{GeV}$	–
	Dijet/missing-p^μ angular separation, $\Delta R_{jj,\text{miss}}$[9]	$\in [3.1, 4.0]$[10]	–
	Dijet azimuthal separation, $\Delta\phi_{jj}$	$> 1.25\,\text{rad}$	$> 1.75\,\text{rad}$
	Leading lepton momentum, p_{ℓ_0}	–	$\in [40, 90]\,\text{GeV}$
	Subleading lepton momentum, p_{ℓ_1}	–	$\in [20, 60]\,\text{GeV}$
	Dilepton mass, $M_{\ell\bar{\ell}}$	–	$\in [80, 100]\,\text{GeV}$
	Dilepton energy, $E_{\ell\bar{\ell}}$	–	$\in [85, 115]\,\text{GeV}$
	Recoil mass, M_{recoil}[11]	–	$\in [122, 155]\,\text{GeV}$
$h \to b\bar{b}/c\bar{c}$ rejection	Leading jet LCFIPlus BTag score, $\text{score}_b^{j_0}$	< 0.20	< 0.1
	Subleading jet LCFIPlus BTag score, $\text{score}_b^{j_1}$	< 0.20	< 0.1
	Leading jet LCFIPlus CTag score, $\text{score}_c^{j_0}$	< 0.35	< 0.3
	Subleading jet LCFIPlus CTag score, $\text{score}_c^{j_1}$	< 0.35	< 0.3
$4f$ VV rejection	$2 \to 3$ jet transition variable, y_{23}[12]	< 0.010	< 0.050
	$3 \to 4$ jet transition variable, y_{34}	< 0.002	< 0.005
$h \to gg$ rejection	Number of PFOs in event, $N_{\text{PFOs}}^{\text{event}}$	$\in [30, 60]$	$\in [20, 80]$
	Number of PFOs in leading jet, $N_{\text{PFOs}}^{j_0}$	$\in [10, 40]$	$\in [5, 40]$
	Number of PFOs in subleading jet, $N_{\text{PFOs}}^{j_1}$	$\in [9, 37]$	$\in [5, 40]$

Cutflows for $h \to ss$ analysis

$Z \to \nu\nu$ channel

ILD Preliminary, $\mathcal{L} = 900$ fb^{-1}, $\sqrt{s} = 250$ GeV, $P(e^-, e^+) = (-80\%, +30\%)$

	$(H \to s\bar{s})(Z \to \ell\ell/\nu\nu)$	$(H \to gg)(Z \to \ell\ell/\nu\nu)$	$(H \to u\bar{u}/d\bar{d})(Z \to \ell\ell/\nu\nu)$	$(H \to c\bar{c})(Z \to \ell\ell/\nu\nu)$	$(H \to b\bar{b})(Z \to \ell\ell/\nu\nu)$	$(H \to \text{other})(Z \to \ell\ell)$	$2f$ Z hadr.	$4f$ ZZ hadr.	$4f$ WW hadr.	$4f$ ZZ/WW hadr.	$2f$ Z lept.	$4f$ ZZ semilept.	$4f$ single Z semilept.	Total bkg.	Sig. eff.	Bkg. eff.
No cut	16.98 ± 0.30	6870 ± 9	0.03 ± 0.00	2333 ± 4	46252 ± 46	8364 ± 12	67373852 ± 13380	739764 ± 278	7827170 ± 2035	6364669 ± 1498	11169172 ± 2257	441249 ± 215	668607 ± 268	94648302 ± 13810	1.00e+00	1.00e+00
No leptons	12.71 ± 0.16	5185 ± 7	0.03 ± 0.00	1757 ± 3	34699 ± 44	1650 ± 5	66784536 ± 13322	736026 ± 277	7793463 ± 2031	6337386 ± 1495	4928498 ± 1499	224163 ± 153	266344 ± 169	87113708 ± 13646	7.49e-01	9.20e-01
≥ 2 jets	12.71 ± 0.16	5185 ± 7	0.03 ± 0.00	1757 ± 3	34699 ± 44	1636 ± 5	66784506 ± 13322	736026 ± 277	7793463 ± 2031	6337386 ± 1495	4693848 ± 1463	224163 ± 153	266343 ± 169	86879015 ± 13642	7.49e-01	9.18e-01
$p_{j_0} \in [40, 110]$ GeV	12.48 ± 0.15	5137 ± 7	0.03 ± 0.00	1735 ± 3	34324 ± 44	1242 ± 5	41461359 ± 10496	660260 ± 262	6685047 ± 1881	5454727 ± 1387	1046002 ± 691	181412 ± 138	107346 ± 107	55638592 ± 10780	7.35e-01	5.88e-01
$p_{j_1} \in [30, 80]$ GeV	11.49 ± 0.14	4874 ± 7	0.03 ± 0.00	1655 ± 3	32362 ± 43	975.14 ± 4.18	28243535 ± 8663	264679 ± 166	1616241 ± 925	1375375 ± 696	137674 ± 251	133869 ± 119	39669 ± 65	31850908 ± 8747	6.77e-01	3.37e-01
$M_{jj} \in [120, 140]$ GeV	8.44 ± 0.10	3523 ± 6	0.02 ± 0.00	1105 ± 2	18299 ± 32	309.59 ± 2.36	2230118 ± 2434	4237 ± 21	57201 ± 174	45988 ± 127	13421 ± 78	18772 ± 44	5234 ± 24	2398207 ± 2446	4.97e-01	2.53e-02
$E_{jj} \in [125, 155]$ GeV	8.30 ± 0.10	3474 ± 6	0.02 ± 0.00	1089 ± 2	18015 ± 32	297.47 ± 2.31	820110 ± 1476	2297 ± 15	27118 ± 120	21885 ± 88	11976 ± 74	11720 ± 35	4054 ± 21	922034 ± 1487	4.89e-01	9.74e-03
$M_{\text{miss}} \in [75, 120]$ GeV	7.81 ± 0.10	3273 ± 6	0.02 ± 0.00	1026 ± 2	17025 ± 31	267.03 ± 2.19	334159 ± 942	1151 ± 11	12273 ± 81	9836 ± 59	9671 ± 66	6383 ± 26	2911 ± 18	397974 ± 951	4.60e-01	4.20e-03
$\Delta R_{jj,\text{miss}} \in [3.1, 4.0]$	6.65 ± 0.08	2819 ± 5	0.02 ± 0.00	884.18 ± 1.92	14664 ± 29	228.21 ± 2.02	55896 ± 385	814.17 ± 9.21	9657 ± 71	7695 ± 52	4074 ± 43	3955 ± 20	232.00 ± 4.98	100919 ± 400	3.92e-01	1.07e-03
$\Delta\phi_{jj} > 1.25$ rad	6.27 ± 0.08	2617 ± 5	0.02 ± 0.00	832.85 ± 1.87	13796 ± 28	205.17 ± 1.92	50100 ± 365	734.35 ± 8.75	8567 ± 67	6818 ± 49	3483 ± 40	3589 ± 19	197.20 ± 4.59	90939 ± 378	3.70e-01	9.61e-04
$\text{score}^{j_0}_{b\text{-tag}} < 0.20$	6.07 ± 0.08	2386 ± 5	0.02 ± 0.00	646.42 ± 1.63	1180 ± 8	158.35 ± 1.68	33593 ± 299	409.22 ± 6.53	7383 ± 63	5887 ± 46	2358 ± 33	2442 ± 16	163.59 ± 4.18	56608 ± 311	3.58e-01	5.98e-04
$\text{score}^{j_1}_{b\text{-tag}} < 0.20$	5.86 ± 0.08	2239 ± 5	0.02 ± 0.00	505.46 ± 1.44	125.64 ± 2.71	130.02 ± 1.53	29249 ± 279	331.69 ± 5.88	6349 ± 58	5202 ± 43	1730 ± 28	1992 ± 14	142.60 ± 3.91	47996 ± 290	3.45e-01	5.07e-04
$\text{score}^{j_0}_{c\text{-tag}} < 0.35$	5.62 ± 0.07	2116 ± 5	0.02 ± 0.00	179.53 ± 0.86	64.57 ± 1.94	97.61 ± 1.32	25178 ± 259	283.55 ± 5.44	4847 ± 51	4381 ± 39	703.89 ± 17.91	1551 ± 13	129.65 ± 3.73	39532 ± 268	3.31e-01	4.18e-04
$\text{score}^{j_1}_{c\text{-tag}} < 0.35$	5.43 ± 0.07	2008 ± 4	0.02 ± 0.00	73.71 ± 0.54	36.71 ± 1.46	74.18 ± 1.15	23060 ± 248	256.56 ± 5.17	3485 ± 43	3782 ± 37	382.03 ± 13.20	1142 ± 11	117.87 ± 3.55	34418 ± 255	3.20e-01	3.64e-04
$y_{23} < 0.010$	3.54 ± 0.06	732.75 ± 2.66	0.01 ± 0.00	41.55 ± 0.40	15.75 ± 0.96	2.56 ± 0.21	8277 ± 148	29.91 ± 1.77	277.83 ± 12.13	342.83 ± 11.00	346.02 ± 12.56	297.66 ± 5.59	43.57 ± 2.16	10408 ± 150	2.08e-01	1.10e-04
$y_{34} < 0.002$	3.06 ± 0.06	397.00 ± 1.96	0.01 ± 0.00	33.87 ± 0.37	11.29 ± 0.82	0.61 ± 0.10	6399 ± 130	12.40 ± 1.14	129.65 ± 8.28	167.89 ± 7.70	338.72 ± 12.43	212.24 ± 4.72	32.33 ± 1.86	7735 ± 132	1.80e-01	8.17e-05
$N^{\text{event}}_{\text{PFOs}} \in [30, 60]$	2.56 ± 0.05	121.22 ± 1.07	0.01 ± 0.00	25.42 ± 0.31	5.64 ± 0.58	0.32 ± 0.08	4831 ± 113	5.63 ± 0.77	63.50 ± 5.80	88.88 ± 5.60	115.34 ± 7.25	163.07 ± 4.14	25.05 ± 1.64	5445 ± 114	1.50e-01	5.75e-05
$N^{j_0}_{\text{PFOs}} \in [10, 40]$	2.48 ± 0.05	117.16 ± 1.05	0.01 ± 0.00	24.90 ± 0.31	5.58 ± 0.58	0.32 ± 0.08	4515 ± 110	5.42 ± 0.75	61.39 ± 5.70	86.76 ± 5.53	92.09 ± 6.48	155.71 ± 4.04	18.41 ± 1.40	5082 ± 110	1.46e-01	5.37e-05
$N^{j_1}_{\text{PFOs}} \in [9, 37]$	2.41 ± 0.05	113.59 ± 1.04	0.01 ± 0.00	24.28 ± 0.30	5.15 ± 0.55	0.32 ± 0.08	4238 ± 106	5.31 ± 0.74	58.74 ± 5.58	85.35 ± 5.49	81.60 ± 6.10	147.20 ± 3.93	15.10 ± 1.27	4775 ± 107	1.42e-01	5.05e-05

$Z \to \ell\ell$ channel

ILD Preliminary, $\mathcal{L} = 900$ fb^{-1}, $\sqrt{s} = 250$ GeV, $P(e^-, e^+) = (-80\%, +30\%)$

	$(h \to s\bar{s})(Z \to \ell\ell/\nu\nu)$	$(h \to gg)(Z \to \ell\ell/\nu\nu)$	$(h \to u\bar{u}/d\bar{d})(Z \to \ell\ell/\nu\nu)$	$(h \to c\bar{c})(Z \to \ell\ell/\nu\nu)$	$(h \to b\bar{b})(Z \to \ell\ell/\nu\nu)$	$(h \to \text{other})(Z \to \ell\ell)$	$2f$ Z hadr.	$4f$ ZZ hadr.	$4f$ WW hadr.	$4f$ ZZ/WW hadr.	$2f$ Z lept.	$4f$ ZZ semilept.	$4f$ single Z semilept.	Total bkg.	Sig. eff.	Bkg. eff.
No cut	16.98 ± 0.30	6870 ± 9	0.03 ± 0.00	2333 ± 4	46252 ± 46	8364 ± 12	67373852 ± 13380	739764 ± 278	7827170 ± 2035	6364669 ± 1498	11169172 ± 2257	441249 ± 215	668607 ± 268	94648302 ± 13810	1.00e+00	1.00e+00
≥ 2 leptons	3.30 ± 0.23	1341 ± 5	0.00 ± 0.00	454.35 ± 2.89	9060 ± 13	5277 ± 10	5190 ± 117	22.93 ± 1.55	210.62 ± 10.56	164.71 ± 7.62	4721316 ± 1467	112061 ± 109	157854 ± 130	5012950 ± 1482	1.95e-01	5.30e-02
Leading 2 leptons are SFOS	3.22 ± 0.22	1324 ± 5	0.00 ± 0.00	448.46 ± 2.87	8928 ± 13	4482 ± 9	3125 ± 91	14.48 ± 1.23	127.01 ± 8.20	93.11 ± 5.73	4655296 ± 1457	110576 ± 108	150905 ± 127	4935320 ± 1469	1.89e-01	5.21e-02
≥ 2 jets	3.22 ± 0.22	1324 ± 5	0.00 ± 0.00	448.46 ± 2.87	8928 ± 13	4457 ± 9	3125 ± 91	14.48 ± 1.23	127.01 ± 8.20	93.11 ± 5.73	4393306 ± 1415	110576 ± 108	150905 ± 127	4673305 ± 1428	1.89e-01	4.94e-02
$p_{j_0} \in [60, 105]$ GeV	3.13 ± 0.22	1198 ± 5	0.00 ± 0.00	416.89 ± 2.77	7910 ± 12	1716 ± 6	1398 ± 61	11.57 ± 1.10	88.91 ± 6.86	65.60 ± 4.81	51478 ± 153	87109 ± 96	97125 ± 102	248516 ± 217	1.84e-01	2.63e-03
$p_{j_1} \in [35, 75]$ GeV	2.96 ± 0.21	1069 ± 5	0.00 ± 0.00	386.41 ± 2.67	7048 ± 11	1112 ± 5	749.35 ± 44.62	4.38 ± 0.68	24.87 ± 3.63	15.52 ± 2.34	1843 ± 29	48889 ± 72	50418 ± 73	111559 ± 116	1.74e-01	1.18e-03
$M_{jj} \in [115, 145]$ GeV	2.52 ± 0.20	900.19 ± 4.14	0.00 ± 0.00	320.55 ± 2.43	5632 ± 10	820.10 ± 3.87	106.29 ± 16.81	0.00 ± 0.00	1.59 ± 0.92	0.35 ± 0.35	515.15 ± 15.32	9311 ± 31	13361 ± 38	30968 ± 55	1.48e-01	3.27e-04
$E_{jj} \in [130, 156]$ GeV	2.46 ± 0.20	846.38 ± 4.01	0.00 ± 0.00	294.41 ± 2.33	4967 ± 9	761.78 ± 3.73	55.80 ± 12.18	0.00 ± 0.00	1.06 ± 0.75	0.00 ± 0.00	339.63 ± 12.44	7152 ± 27	10353 ± 33	24770 ± 48	1.45e-01	2.62e-04
$\Delta\phi_{jj} > 1.75$ rad	2.13 ± 0.18	743.14 ± 3.76	0.00 ± 0.00	265.33 ± 2.21	4455 ± 9	635.11 ± 3.40	45.17 ± 10.96	0.00 ± 0.00	0.00 ± 0.00	0.00 ± 0.00	191.47 ± 9.34	5377 ± 24	8098 ± 29	19810 ± 42	1.25e-01	2.09e-04
$p_{\ell_0} \in [40, 90]$ GeV	2.12 ± 0.18	733.97 ± 3.74	0.00 ± 0.00	261.92 ± 2.19	4400 ± 9	626.17 ± 3.38	15.94 ± 6.51	0.00 ± 0.00	0.00 ± 0.00	0.00 ± 0.00	80.24 ± 6.05	4623 ± 22	6785 ± 27	17527 ± 37	1.25e-01	1.85e-04
$p_{\ell_1} \in [20, 60]$ GeV	2.10 ± 0.18	722.56 ± 3.71	0.00 ± 0.00	257.41 ± 2.17	4320 ± 9	615.67 ± 3.35	13.29 ± 5.94	0.00 ± 0.00	0.00 ± 0.00	0.00 ± 0.00	62.00 ± 5.32	4336 ± 21	5938 ± 25	16264 ± 36	1.24e-01	1.72e-04
$M_{\ell\ell} \in [80, 100]$ GeV	1.86 ± 0.17	640.71 ± 3.49	0.00 ± 0.00	228.19 ± 2.05	3822 ± 8	544.79 ± 3.15	10.63 ± 5.31	0.00 ± 0.00	0.00 ± 0.00	0.00 ± 0.00	46.04 ± 4.58	3246 ± 18	3328 ± 19	11867 ± 29	1.10e-01	1.25e-04
$E_{\ell\ell} \in [85, 115]$ GeV	1.86 ± 0.17	636.54 ± 3.48	0.00 ± 0.00	226.73 ± 2.04	3798 ± 8	541.07 ± 3.14	7.97 ± 4.60	0.00 ± 0.00	0.00 ± 0.00	0.00 ± 0.00	25.07 ± 3.38	1988 ± 14	2163 ± 15	9386 ± 24	1.10e-01	9.92e-05
$M_{\text{recoil}} \in [122, 155]$ GeV	1.85 ± 0.17	632.19 ± 3.46	0.00 ± 0.00	224.83 ± 2.03	3774 ± 8	537.96 ± 3.13	7.97 ± 4.60	0.00 ± 0.00	0.00 ± 0.00	0.00 ± 0.00	21.88 ± 3.16	1390 ± 12	1423 ± 12	8011 ± 21	1.09e-01	8.46e-05
$\text{score}_{b\text{-tag}j_0} < 0.1$	1.62 ± 0.16	544.39 ± 3.21	0.00 ± 0.00	133.66 ± 1.57	185.87 ± 1.83	378.73 ± 2.63	5.31 ± 3.76	0.00 ± 0.00	0.00 ± 0.00	0.00 ± 0.00	18.69 ± 2.92	973.89 ± 10.12	1007 ± 10	3248 ± 16	9.56e-02	3.43e-05
$\text{score}^{j_1}_{b\text{-tag}} < 0.1$	1.49 ± 0.15	480.32 ± 3.02	0.00 ± 0.00	78.23 ± 1.20	17.41 ± 0.56	285.53 ± 2.28	2.66 ± 2.66	0.00 ± 0.00	0.00 ± 0.00	0.00 ± 0.00	15.96 ± 2.70	832.36 ± 9.35	851.01 ± 9.55	2563 ± 14	8.75e-02	2.71e-05
$\text{score}^{j_0}_{c\text{-tag}} < 0.3$	1.45 ± 0.15	460.16 ± 2.96	0.00 ± 0.00	30.26 ± 0.75	12.13 ± 0.47	244.09 ± 2.11	2.66 ± 2.66	0.00 ± 0.00	0.00 ± 0.00	0.00 ± 0.00	15.04 ± 2.62	749.46 ± 8.87	778.54 ± 9.13	2292 ± 14	8.55e-02	2.42e-05
$\text{score}^{j_1}_{c\text{-tag}} < 0.3$	1.41 ± 0.15	441.74 ± 2.90	0.00 ± 0.00	14.00 ± 0.51	9.24 ± 0.41	209.58 ± 1.95	2.66 ± 2.66	0.00 ± 0.00	0.00 ± 0.00	0.00 ± 0.00	14.59 ± 2.58	702.60 ± 8.59	733.57 ± 8.86	2128 ± 13	8.29e-02	2.25e-05
$y_{23} < 0.050$	1.35 ± 0.15	374.27 ± 2.67	0.00 ± 0.00	12.63 ± 0.48	8.55 ± 0.39	110.47 ± 1.42	2.66 ± 2.66	0.00 ± 0.00	0.00 ± 0.00	0.00 ± 0.00	14.59 ± 2.58	583.97 ± 7.83	608.63 ± 8.07	1716 ± 12	7.93e-02	1.81e-05
$y_{34} < 0.005$	1.15 ± 0.13	272.26 ± 2.27	0.00 ± 0.00	11.00 ± 0.45	7.29 ± 0.36	27.26 ± 0.70	2.66 ± 2.66	0.00 ± 0.00	0.00 ± 0.00	0.00 ± 0.00	14.59 ± 2.58	490.88 ± 7.18	487.44 ± 7.22	1313 ± 11	6.78e-02	1.39e-05
$N^{\text{event}}_{\text{PFOs}} \in [20, 80]$	1.14 ± 0.13	179.45 ± 1.84	0.00 ± 0.00	10.39 ± 0.44	6.48 ± 0.34	22.61 ± 0.64	2.66 ± 2.66	0.00 ± 0.00	0.00 ± 0.00	0.00 ± 0.00	5.93 ± 1.64	474.49 ± 7.06	466.46 ± 7.07	1168 ± 11	6.70e-02	1.23e-05
$N^{j_0}_{\text{PFOs}} \in [5, 40]$	1.04 ± 0.13	128.20 ± 1.56	0.00 ± 0.00	8.87 ± 0.40	5.09 ± 0.30	17.10 ± 0.56	2.66 ± 2.66	0.00 ± 0.00	0.00 ± 0.00	0.00 ± 0.00	4.56 ± 1.44	424.06 ± 6.67	415.39 ± 6.67	1006 ± 10	6.14e-02	1.06e-05
$N^{j_1}_{\text{PFOs}} \in [5, 40]$	1.04 ± 0.13	102.30 ± 1.39	0.00 ± 0.00	8.06 ± 0.38	4.68 ± 0.29	14.48 ± 0.51	2.66 ± 2.66	0.00 ± 0.00	0.00 ± 0.00	0.00 ± 0.00	4.56 ± 1.44	396.95 ± 6.46	384.66 ± 6.42	918.35 ± 9.72	6.14e-02	9.70e-06

Cutflow discussion

The cutflow for the $Z \to \nu\bar{\nu}$ channel is shown in Table 4. Histograms of the variables included as part of this channel's selections (showing the evolution of the yields as each selection is applied) are shown in Figs. 8 through 11. From Table 4, we see the signal efficiency for our selections is 14% while our background efficiency is 0.005%. Even with the high background rejection, $Z \to q\bar{q}$ is still highly dominant with ∼4,200 events compared to the ∼2 events expected for $h \to s\bar{s}$. Therefore, improvements to the sensitivity of the analysis are expected to be accompanied by improved rejection of $Z \to q\bar{q}$. The $h \to gg$ process is the dominant Higgs background with ∼110 events.

The cutflow for the $Z \to \ell\bar{\ell}$ channel is shown in Table 5. Histograms of the variables included as part of this channel's selections (showing the evolution of the yields as each selection is applied) are shown in Figs. 12 through 16. From Table 5, the hadronic backgrounds are almost entirely removed by cutting on the number of leptons. The signal efficiency for our selections is 6% while our background efficiency is 0.001%. The $4f$ single Z and ZZ backgrounds are the dominant backgrounds, with ∼800 events compared to the ∼1 events expected for $h \to s\bar{s}$. As with the $Z \to \nu\bar{\nu}$ channel, the $h \to gg$ process is the dominant Higgs background with ∼100 events.

Limit plots on κ_s from $h \to ss$ analysis

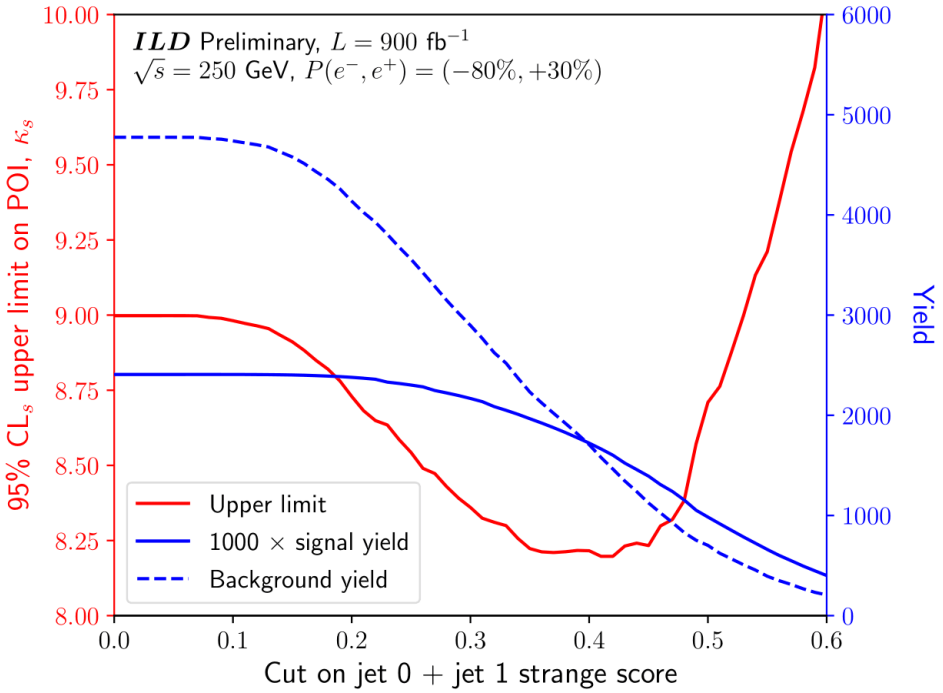

$Z \to \nu\nu$ channel

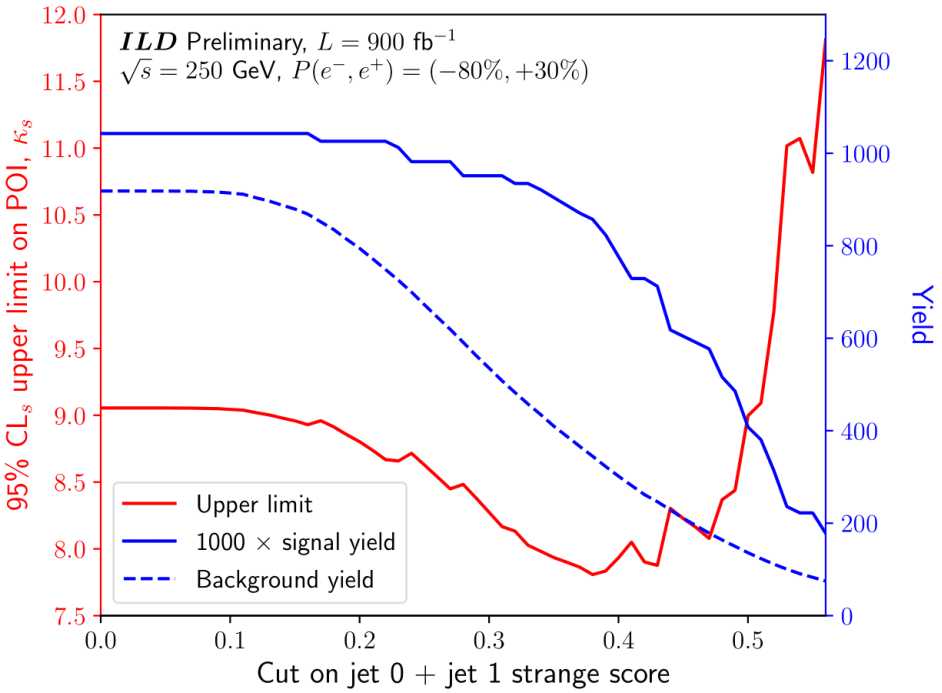

$Z \to ll$ channel

Limits on κ_s when PID is *absent*

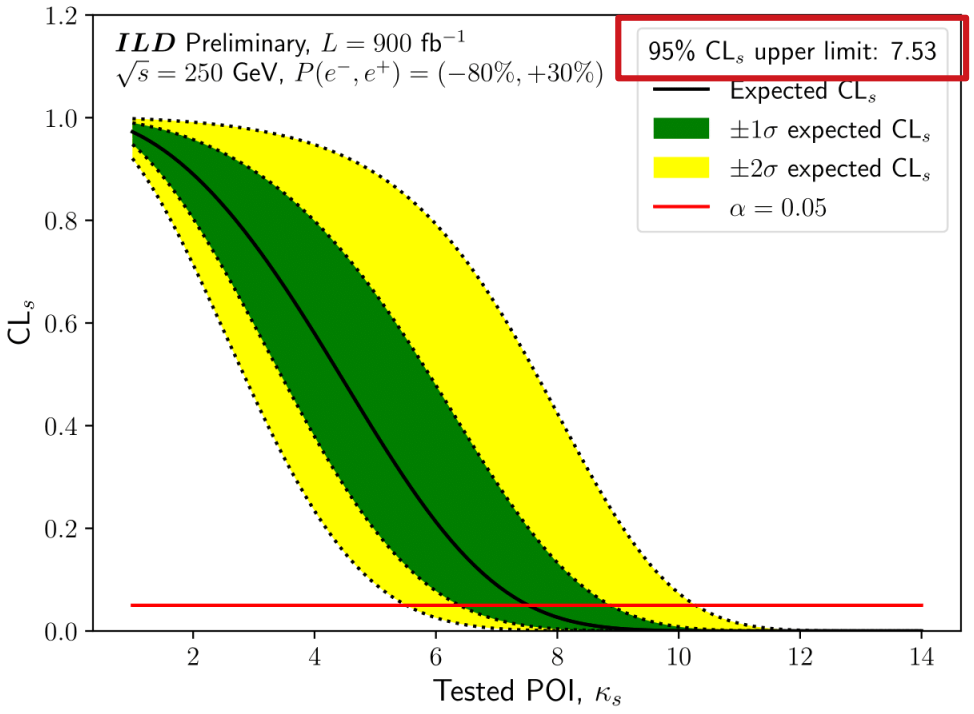

Compared to 6.74 with full PID

RICH: estimated performance for different particle types and momenta

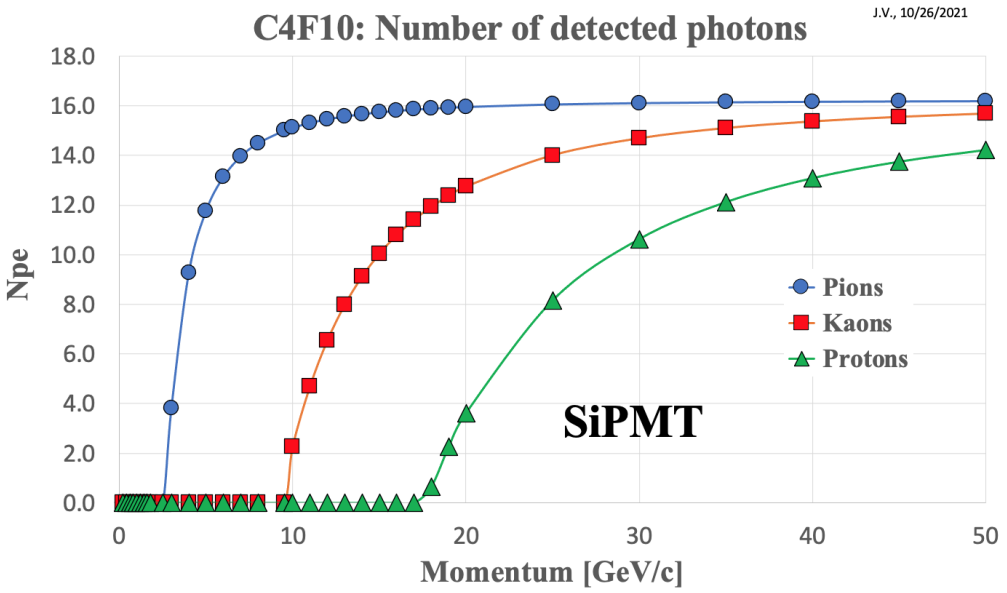

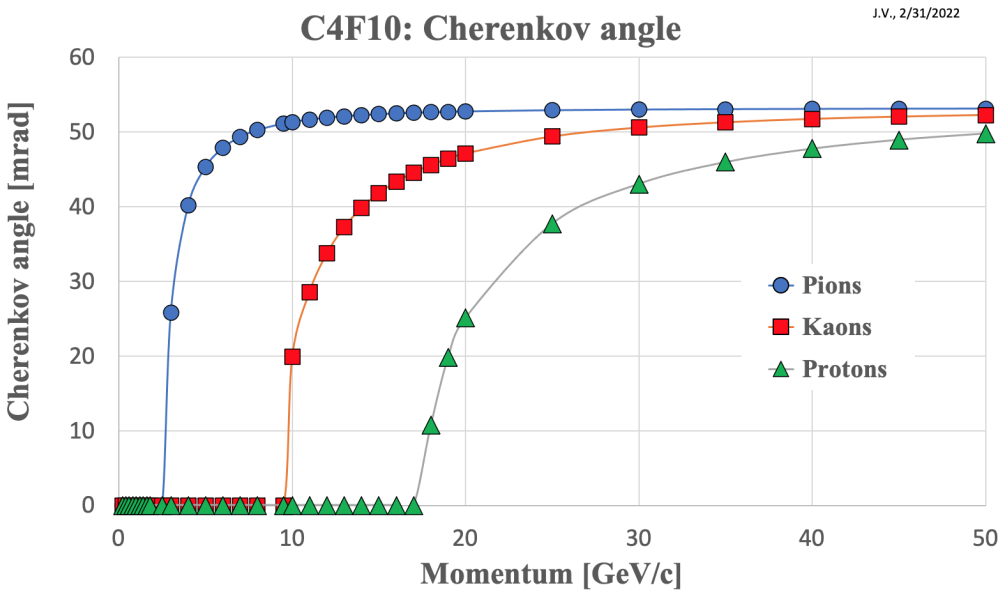

RICH: helix trajectories and ray tracing

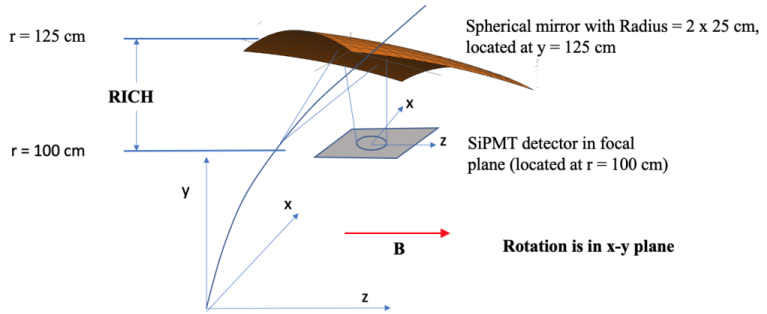

(a)

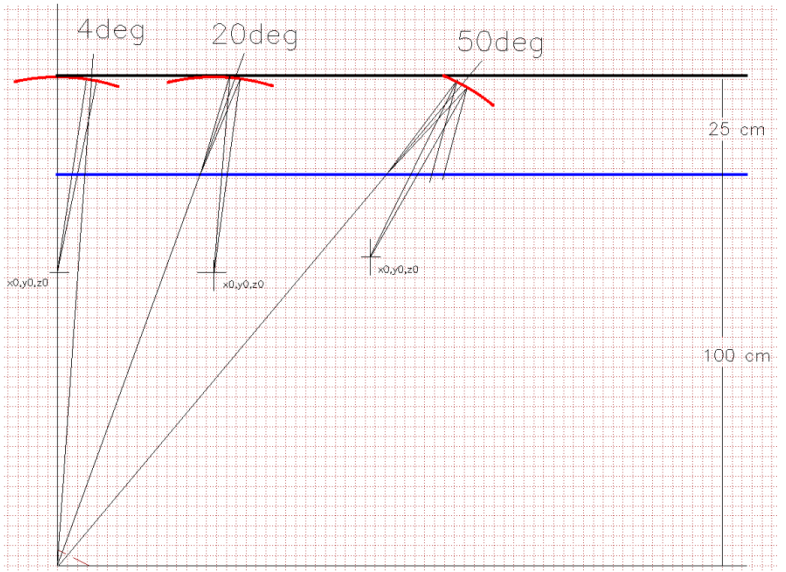

(b)

Figure 27: (a) A schematic diagram of the helix trajectory and Cherenkov cone. Notice that cones move in 3D. A simple program was implemented: step through the magnetic field, radiate Cherenkov photons when $100 < r < 125\,\text{cm}$, reflect them from a spherical mirror, and find their intersection with a detector plane. (b) Ray tracing model for the simulation of three dip angles.

RICH: Cherenkov rings for varying dip angle

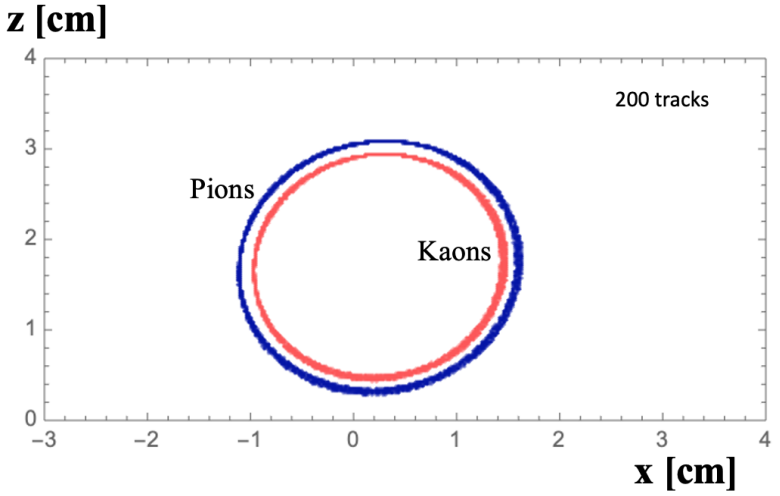

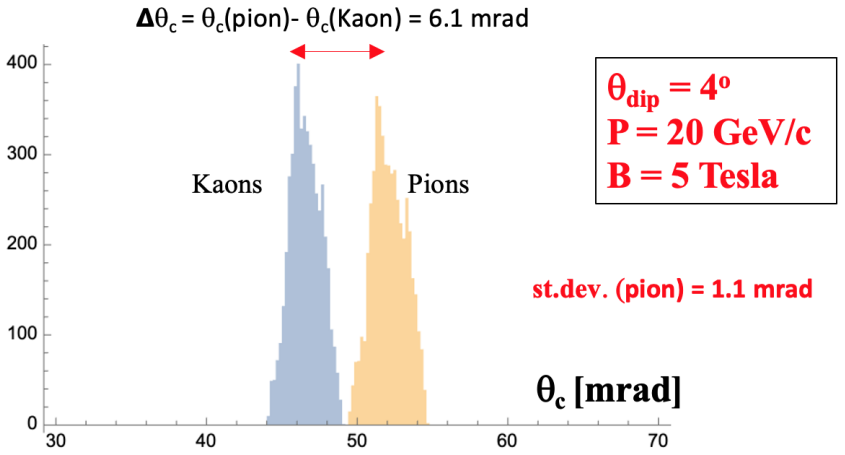

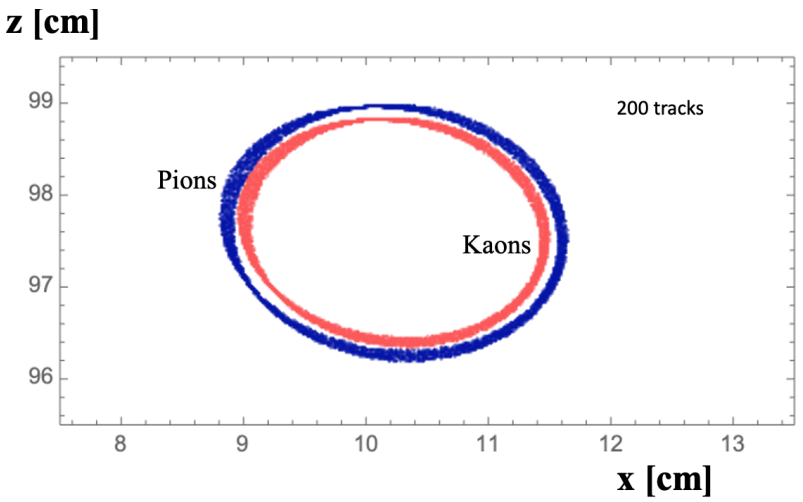

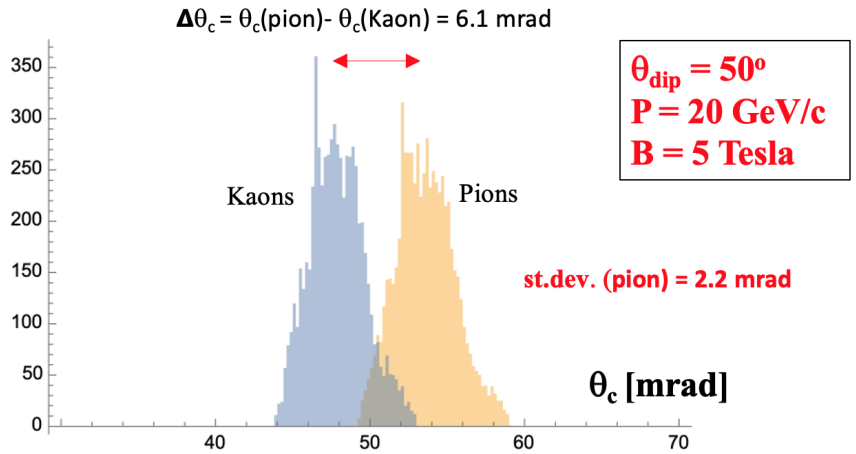

RICH: Cherenkov rings for varying momentum

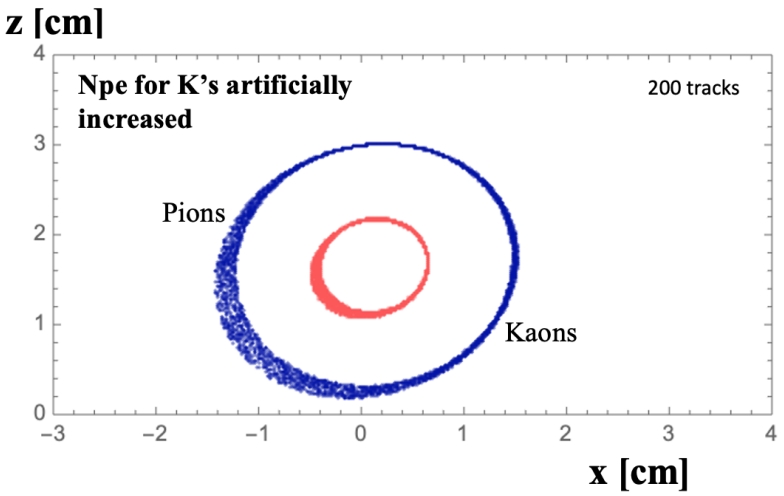

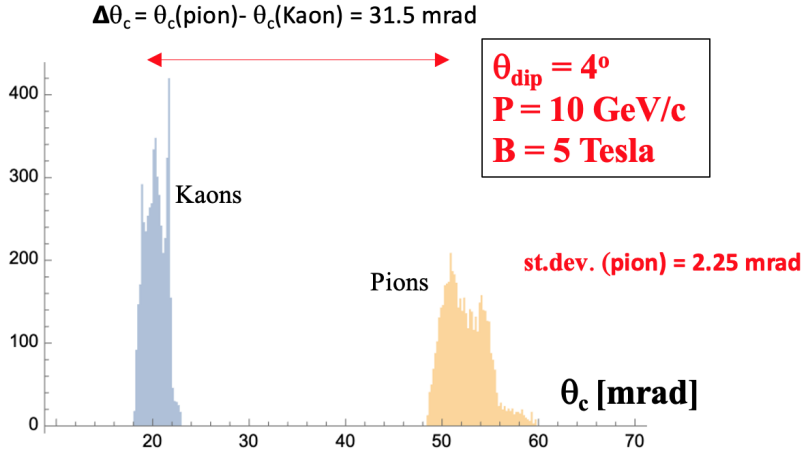

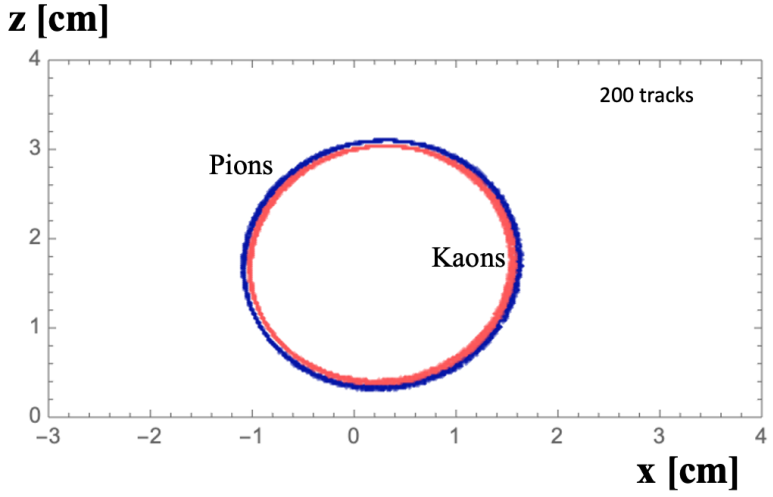

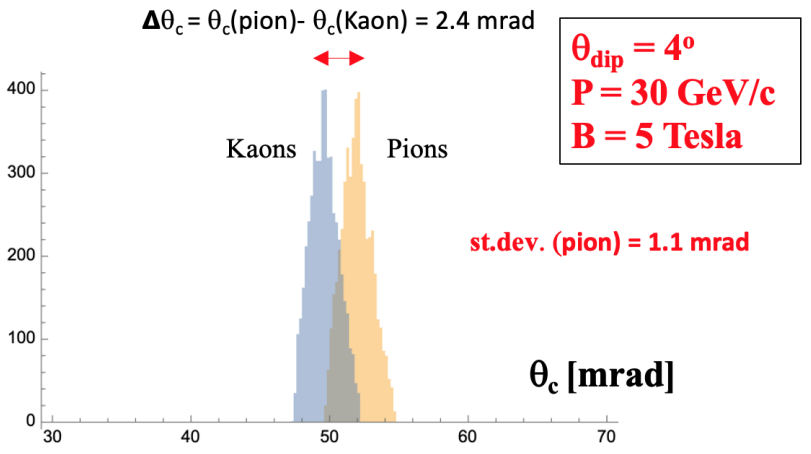

RICH: contributions to the Cherenkov angle resolution

Table 6: Various contributions to the Cherenkov angle resolution.

Single photon error source	SiD/ILD RICH detector [mrad]	SLD CRID detector [mrad]
Chromatic error	$\sim$0.9	$\sim$0.4
Pixel size error (1–3 mm^2)	0.8–2.3	$\sim$0.5
Smearing effect due to magnetic field	1.5–2.5	$\sim$0.5
Mirror alignment	< 1	$\sim$1
Tracking angular error	< 1	$\sim$0.8 [93, 94]
Other systematics errors	a few mrad	a few mrad
Total	< 5	$\sim$4.3

RICH: Performance versus other PID methods